



**HAL**  
open science

## Combining neuroanatomical features to support diagnosis of fetal alcohol spectrum disorders

Justine Fraize, Pauline Garzón, Alexandra Ntorkou, Eliot Kerdreux, Odile Boespflug-Tanguy, Anita Beggiato, Richard Delorme, Lucie Hertz-Pannier, Monique Elmaleh-Berges, David Germanaud

### ► To cite this version:

Justine Fraize, Pauline Garzón, Alexandra Ntorkou, Eliot Kerdreux, Odile Boespflug-Tanguy, et al.. Combining neuroanatomical features to support diagnosis of fetal alcohol spectrum disorders. *Developmental Medicine and Child Neurology*, 2022, Online ahead of print. 10.1111/dmcn.15411 . inserm-03828534

**HAL Id: inserm-03828534**

**<https://inserm.hal.science/inserm-03828534v1>**

Submitted on 25 Oct 2022

**HAL** is a multi-disciplinary open access archive for the deposit and dissemination of scientific research documents, whether they are published or not. The documents may come from teaching and research institutions in France or abroad, or from public or private research centers.

L'archive ouverte pluridisciplinaire **HAL**, est destinée au dépôt et à la diffusion de documents scientifiques de niveau recherche, publiés ou non, émanant des établissements d'enseignement et de recherche français ou étrangers, des laboratoires publics ou privés.

See discussions, stats, and author profiles for this publication at: <https://www.researchgate.net/publication/363776532>

# Combining neuroanatomical features to support diagnosis of fetal alcohol spectrum disorders

Article in *Developmental Medicine & Child Neurology* · September 2022

DOI: 10.1111/dmcn.15411

CITATIONS

0

READS

13

10 authors, including:



**Justine Fraize**

French Institute of Health and Medical Research

1 PUBLICATION 0 CITATIONS

[SEE PROFILE](#)



**Eliot Kerdreux**

French Institute of Health and Medical Research

1 PUBLICATION 0 CITATIONS

[SEE PROFILE](#)



**Anita Beggiano**

Assistance Publique – Hôpitaux de Paris

47 PUBLICATIONS 880 CITATIONS

[SEE PROFILE](#)



**Richard Delorme**

Hôpital Universitaire Robert Debré

281 PUBLICATIONS 12,972 CITATIONS

[SEE PROFILE](#)

Some of the authors of this publication are also working on these related projects:




Autism [View project](#)



Pineal and Melatonin [View project](#)

## ORIGINAL ARTICLE

# Combining neuroanatomical features to support diagnosis of fetal alcohol spectrum disorders

Justine Fraize<sup>1,2</sup>  | Pauline Garzón<sup>1,2</sup> | Alexandra Ntorkou<sup>3</sup> | Eliot Kerdreux<sup>1,2</sup> | Odile Boespflug-Tanguy<sup>4</sup> | Anita Beggiato<sup>5</sup> | Richard Delorme<sup>5</sup> | Lucie Hertz-Pannier<sup>1,2</sup> | Monique Elmaleh-Berges<sup>2,3</sup> | David Germanaud<sup>1,2,6</sup>

<sup>1</sup>CEA Paris-Saclay, Frederic Joliot Institute, NeuroSpin, UNIACT, Gif-sur-Yvette, France

<sup>2</sup>Université Paris Cité, Inserm, NeuroDiderot, InDEV, Paris, France

<sup>3</sup>Department of Paediatric Radiologic, Centre of Excellence InovAND, Robert-Debré Hospital, AP-HP, Paris, France

<sup>4</sup>Université Paris Cité, Inserm, NeuroDiderot, NeuroDEV, Paris, France

<sup>5</sup>Department of Child and Adolescent Psychiatry, Centre of Excellence InovAND, Robert-Debré Hospital, AP-HP, Paris, France

<sup>6</sup>Department of Genetics, Centre of Excellence InovAND, Robert-Debré Hospital, AP-HP, Paris, France

## Correspondence

Justine Fraize, NeuroSpin, Bâtiment 145, CEA Paris-Saclay, 91191 Gif-sur-Yvette, France.  
Email: [justine.fraize@inserm.fr](mailto:justine.fraize@inserm.fr)

## Funding information

French National Agency for Research, Grant/Award Number: ANR-19-CE17-0028-01; French National Institute for Public Health research, Grant/Award Number: IRESP-19-ADDICTIONS-08

## Abstract

**Aim:** To identify easily accessible neuroanatomical abnormalities useful for diagnosing fetal alcohol spectrum disorders (FASD) in fetal alcohol syndrome (FAS) but more importantly for the probabilistic diagnosis of non-syndromic forms (NS-FASD).

**Method:** We retrospectively collected monocentric data from 52 individuals with FAS, 37 with NS-FASD, and 94 paired typically developing individuals (6–20 years, 99 males, 84 females). On brain T1-weighted magnetic resonance imaging, we measured brain size, corpus callosum length and thicknesses, vermis height, then evaluated vermis foliation (Likert scale). For each parameter, we established variations with age and brain size in comparison individuals (growth and scaling charts), then identified participants with abnormal measurements (<10th centile).

**Results:** According to growth charts, there was an excess of FAS with abnormally small brain, isthmus, splenium, and vermis. According to scaling charts, this excess remained only for isthmus thickness and vermis height. The vermis foliation was pathological in 18% of those with FASD but in no comparison individual. Overall, 39% of those with FAS, 27% with NS-FASD, but only 2% of comparison individuals presented with two FAS-recurrent abnormalities, and 19% of those with FAS had all three. Considering the number of anomalies, there was a higher likelihood of a causal link with alcohol in 14% of those with NS-FASD.

**Interpretation:** Our results suggest that adding an explicit composite neuroanatomical–radiological criterion for FASD diagnosis may improve its specificity, especially in NS-FASD.

The neurodevelopmental toxicity of ethanol has long been attested by congenital brain abnormalities and the high prevalence of neurodevelopmental disorders following severe prenatal alcohol exposure (PAE).<sup>1</sup> Yet, it remains a

frequent and underdiagnosed cause of cognitive and behavioural disabilities.<sup>2</sup> Grouped under the umbrella diagnosis of fetal alcohol spectrum disorder (FASD), the pathological consequences of PAE range from fetal alcohol

**Abbreviations:** ACC, agenesis of corpus callosum; FAS, fetal alcohol syndrome; FASD, fetal alcohol spectrum disorder; NS-FASD, non-syndromic fetal alcohol spectrum disorder; PAE, prenatal alcohol exposure; RBA, reference brain area (axial).

This is an open access article under the terms of the [Creative Commons Attribution-NonCommercial-NoDerivs](https://creativecommons.org/licenses/by-nc-nd/4.0/) License, which permits use and distribution in any medium, provided the original work is properly cited, the use is non-commercial and no modifications or adaptations are made.

© 2022 The Authors. *Developmental Medicine & Child Neurology* published by John Wiley & Sons Ltd on behalf of Mac Keith Press.

syndrome (FAS) with its specific association of facial features, body, and brain growth deficiency, to non-specific non-syndromic FASD (NS-FASD) when these physical criteria are absent or incomplete, but a probabilistic causal link can be assumed between neurodevelopmental disorders and PAE. Several guidelines for diagnosing FASD have been published<sup>3–5</sup> and revised,<sup>6</sup> which now share a common backbone of key clinical criteria among which the dysmorphic facial features have a well-codified evaluation and a decisive value. The full facial phenotype consensually involves a more specific diagnostic category with a more certain causal link with PAE. The cerebral phenotype is more diversely considered for both the features deemed relevant and their diagnostic significance. Anatomical and functional impairments are either grouped or treated separately depending on guidelines or versions with little impact on diagnosis.

The most patent neuroanatomical abnormality in FASD is a global brain growth deficiency that frequently results in clinical microcephaly.<sup>7,8</sup> More focal brain abnormalities have also been described,<sup>9–11</sup> most of them rarely or hardly apparent on individual magnetic resonance imaging (MRI) scans: abnormalities of the corpus callosum<sup>11–14</sup> or the cerebellum, particularly the vermis,<sup>15–17</sup> or nodular heterotopias. However, neither clinical radiology nor computational imaging findings have so far enabled FASD-relevant brain abnormalities to be unambiguously discriminated from incidental or non-suggestive ones, let alone warranted a consensual well-codified distinct neuroanatomical criterion influencing diagnosis. Currently, any structural brain abnormality of presumed prenatal origin is considered like any severe functional impairment,<sup>4</sup> or given a higher diagnostic weight,<sup>5</sup> or else considered a distinct item, with an emphasis on microcephaly mainly for its frequency-driven practical value,<sup>6</sup> but with little influence on the final diagnosis. Unlike dysmorphic facial features, neuroanatomical abnormalities provide very little,<sup>6</sup> if any,<sup>4,5</sup> etiological specificity in FASD diagnosis, even though the brain is a major target of ethanol developmental toxicity.

In our study, we aimed to characterize recurrent anomalies on brain MRI whose combination could be of diagnostic value in FASD. We first considered measurements of brain size, corpus callosum, and vermis, and compared the individual values observed in FAS with the distributions according to age and then brain size in typically developing comparison individuals, to identify which of these measures were frequently abnormal in individuals with FAS, while not being trivially explained by brain growth deficiency. Beyond vermian height measurement, we established the ability of a semi-quantitative Likert scale, describing the shape of the upper vermis, to accurately distinguish typical from atypical vermis. We then investigated whether individuals with FAS and NS-FASD presented a combination of small brain size with one or more of the callosal and vermian abnormalities we showed to be recurrent in FAS, while comparison individuals did not. Finally, we sought to establish whether

### What this paper adds

- Neuroanatomical anomalies independent of microcephaly can be measured with clinical-imaging tools.
- Small-for-age brain, small-for-brain-size callosal isthmus or vermian height, and disrupted vermis foliation are fetal alcohol syndrome (FAS)-recurrent anomalies.
- Associations of these anomalies are frequent in fetal alcohol spectrum disorder (FASD) even without FAS, while exceptional in typically developing individuals.
- These associations support higher likelihood of causal link with alcohol in some individuals with non-syndromic FASD.
- A new explicit and composite neuroanatomical-radiological criterion can improve the specificity of FASD diagnosis.

taking such combinations into account in the diagnosis could constitute an additional argument to estimate the causal link with PAE.

## METHOD

### Participants

We performed a retrospective case–control study with monocentric recruitment for participants with FASD and bicentric for comparison individuals. Eighty-nine participants with FASD, aged 6 to 20 years, were included among the 149 diagnosed between 2014 and 2020 at Robert-Debré University Hospital (AP-HP, Paris, France) (Figure S1). Ninety-four typically developing comparison individuals aged 6 to 20 years, with no report of PAE nor family history of neurological or psychiatric condition (in first-degree relatives) recruited as part of independent research programmes, were included.

This study was not a clinical trial and the use of previous data sets was approved by the appropriate ethics committees (CER-Paris-Saclay 2020–094 for participants with FASD, Inserm 08–029 and 11–008 for comparison individuals) ensuring proper consent of participants.

### FASD diagnostic procedure

Positive diagnosis was established according to the 4-Digit Diagnostic Code<sup>5</sup> and the revised guidelines of the Institute of Medicine<sup>6</sup> leading to distinguish two groups of FASD: the syndromic or FAS (including partial FAS), and the non-syndromic or NS-FASD (static encephalopathy and

neurobehavioural disorder/alcohol exposed<sup>5</sup> or alcohol-related neurodevelopmental disorder<sup>6</sup>) (Figure S1). Our differential diagnosis work-up included systematic brain MRI and genetic testing. We evaluated the concordance (Cohen's kappa coefficient,  $\kappa$ ) of between-group assignment using one or the other guideline. As it proved to be high in our population, only the 4-Digit Diagnostic Code was used in subsequent analyses.

## MRI data acquisition

MRI acquisitions were performed on a 1.5 Tesla Philips Ingenia MRI scanner (Philips Healthcare, Amsterdam, the Netherlands) with a millimetric isotropic three-dimensional T1-weighted fast field echo–turbo field echo sequence (repetition time = 8.2 ms; echo time = 3.8 ms; inversion time = 0.8 s; Flip = 8°; SENSitivity Encoding [SENSE] = 2) for participants with FASD and 41 scanner-matched comparison individuals, and on a 3 Tesla Siemens Trio MRI scanner (Siemens Healthineers, Oxford, UK) with a millimetric isotropic three-dimensional T1-weighted magnetization prepared rapid gradient-echo sequence for the remaining comparison individuals.<sup>19</sup>

## Neuroanatomical quantitative measurements

Measurements were manually performed using the PACS measurement tools (Carestream, New York, NY, USA) by one operator (J.F.) blind to diagnosis. An axial reference brain area (RBA) (Figure 1a,b) was used as a proxy of brain size, as it is strongly correlated with the actual total brain volume ( $R^2 = 74.9\%$ ; Figure S2). The square root of the RBA was used for the sake of dimensional homogeneity (other measurements being lengths). The length of the corpus callosum, the genu thickness, body thickness, isthmus thickness, splenium thickness, and height of the vermis (Figure 1c–e) were measured according to previously validated methods<sup>20,21</sup> and we ensured that there was no scanner effect in the comparison group (Table S1). For two individuals with obvious partial agenesis of corpus callosum (ACC), the thicknesses were

measured as zero for the agenetic parts. A post hoc robustness analysis excluding these individuals was systematically proposed for callosal parameters.

## Semi-quantitative assessment of upper vermis foliation

A five-point Likert scale was proposed to evaluate the upper vermis foliation (Figure 2). Three experts performed blind and independent ranking of the participants with FASD and the scanner-matched comparison individuals only (to avoid lifting the blind reading process). Observer agreement was assessed with  $\kappa$  considering the five ranks separately and then grouping ranks 1 to 3. The rank finally assigned was the nearest-rounded average of the three observers.

## Modelling and statistical analysis

Statistical analyses were performed in R (R Foundation for Statistical Computing, Vienna, Austria), using packages ‘stats’, ‘graphics’, and ‘irr’. Alpha risk was set at 0.05 and adjusted to 0.007 in the case of multiple comparisons on the seven measured parameters (Bonferroni correction).

The effects of groups or covariates (sex) on quantitative variables were tested by analysis of variance (ANOVA;  $F$ -test) and comparisons of means between two groups were performed with Student's  $t$ -tests. Comparisons of proportions between groups for qualitative variables were performed either with a  $\chi^2$  test (two groups) or proportion test (more).

## Growth and scaling charts in typically developing comparison individuals

The growth relationships between measured parameters ( $P$ ) and age were modelled by a linear law with slope  $a$  and intercept  $b$  ( $P = a \times \text{age} + b$ ), justified by asymptotically linear growth after 6 years old already described in the typically developing paediatric population.<sup>20,21</sup> The scaling

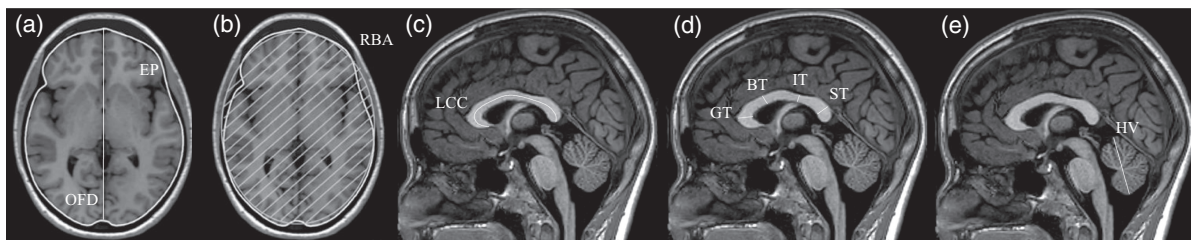


**FIGURE 1** Neuroanatomical quantitative measurements. (a) Encephalic perimeter (EP), occipitofrontal diameter (OFD) on the axial referential section through the anterior and posterior commissures. (b) Reference brain area  $\left( RBA = \pi \cdot OFD \cdot d; EP \approx 2\pi \sqrt{\frac{OFD^2 + d^2}{2}} \right)$ ,  $d$  being an intermediate

parameter corresponding to the smaller of the two diameters of the ellipse (the other being the OFD). (c) Length of the corpus callosum (LCC). (d) Genu thickness (GT), body thickness (BT), isthmus thickness (IT), and splenium thickness (ST). (e) Height of the vermis (HV).



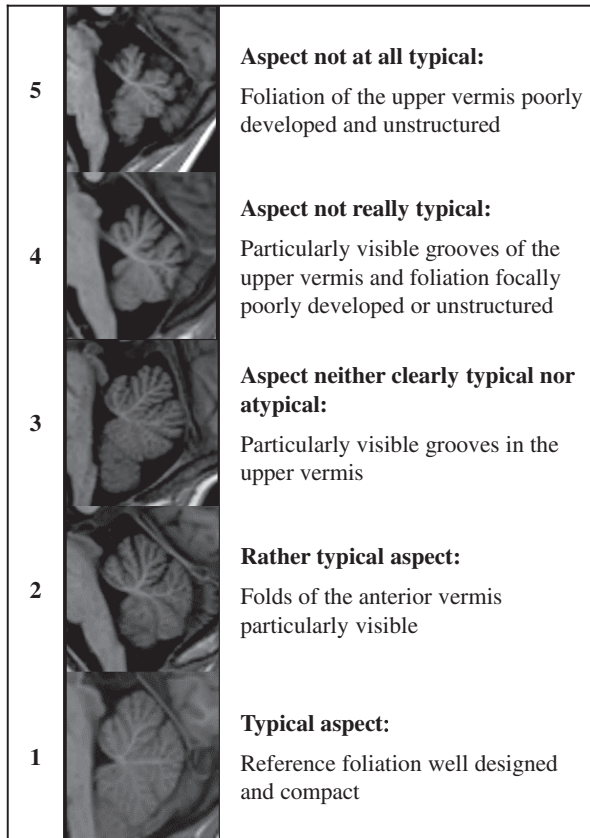


**FIGURE 2** Five-point Likert scale of upper vermis foliation. Anterior vermis: up to and including the primary fissure; upper vermis: above the horizontal fissure. Examples are 'medium' for their rank. Assessment was performed on median sagittal and left/right  $-1/-2$  sections; overall size of the vermis was not considered per se.

relationships between measured parameters ( $P$ ) and brain size (RBA) were modelled by a power law with scaling coefficient  $a$  and constant  $b$  ( $P = b \times \sqrt{\text{RBA}}^a$ ) to take into account expected allometric effects<sup>22,23</sup> (changes in proportions with size). For each measured parameter, we established growth and scaling normative charts by fitting those two models in the comparison group, then estimated the 10th centile curve under the assumption of homogeneous variance along the age or brain size interval. We tested age or brain size effect by comparing the fitted models with constant model ( $F$ -test, nested models) and estimated the part of variance of  $P$  explained by age or brain size with the coefficient of determination ( $R^2$ ). As an alternative analysis, we also established charts in male and female groups.

### Abnormal measurement detection in participants with FASD (normative analysis)

For each parameter, individuals with measurements below the 10th centile curve were counted as normatively too small for age or for brain size. An FAS-recurrent abnormality was considered when the number of too-small measurements in FAS exceeded the theoretically expected 10% of the

individuals (one-sided Fisher's test) and were finally retained only if persistent for brain size (with scaling charts). Lastly, the number of participants with FAS and NS-FASD presenting with combinations of these FAS-recurrent abnormalities was compared with the typically developing individuals to assess the discriminative value.

### Neuroanatomical diagnostic criteria and probabilistic link with PAE

We incorporated the combination of FAS-recurrent neuroanatomical abnormalities in a radiological-clinical diagnostic criterion, both explicit and quantitative, inspired by the revised Institute of Medicine decision tree and the 4-Digit Diagnostic Code severity ranking. Assuming that the greater the number of recurrent abnormalities observed in an individual with FASD, the stronger the probabilistic causal link with PAE, we also associated the different combinations of non-facial criteria with a six-level scale of causal link ranging from unlikely to certain. We finally sought how many participants with NS-FASD had a high probability.

## RESULTS

### Population

Among the 89 participants with FASD, 58.4% had FAS and 41.6% had NS-FASD. Their clinical characteristics are detailed in Table 1. There was no significant group effect for sex ratio ( $p = 0.179$ ) and mean age ( $p = 0.140$ ). The 4-Digit Diagnostic Code and revised Institute of Medicine guidelines were discordant only for six individuals (6.7%,  $\kappa = 0.86$ ), with no effect on further results (Table 1).

### Comparison of mean measurements

There were group differences for all measurements except the genu thickness ( $p = 0.063$ ), even after excluding the two with ACC (data not shown), and we found no sex effect. The NS-FASD group's measurements were intermediate between comparison individuals and the group with FAS. FAS and NS-FASD groups differed only for height of the vermis measurements ( $p = 0.002$ ) (Table 2).

### Growth deficiency: individual measurements as a function of age

In the 94 comparison individuals, callosal and vermian measurements did not change significantly with age, except for the splenium thickness ( $p = 0.003$ ); the determination coefficient  $R^2$  was always lower than 10% (Figure S3). Among the 89 participants with FASD, brain size (RBA) was below the 10th centile of comparison individuals in 74.2%

**TABLE 1** Sociodemographic, clinical, radiological, and functional characteristics of participants with FASD and comparison individuals, and group comparison

	FAS <i>n</i> = 52	NS-FASD <i>n</i> = 37	Typically developing <i>n</i> = 94	Group comparison	
				Group effect, <i>p</i> <sup>a</sup>	FAS vs NS-FASD, <i>p</i> <sup>b</sup>
Sociodemographic assessment					
Sex (% male)	27 (51.9)	25 (67.6)	47 (50.0)	0.179	0.209
Age at first consultation, mean (SD), years:months	10:4 (3:8)	11:4 (3:11)	—	—	0.217
Age at MRI, mean (SD), years:months	10:1 (3:7)	11:11 (3:7)	12:1 (3:5)	0.140	0.219
Adopted (%)	32 (61.5)	22 (59.5)	0 (0.0)	<b>&lt;0.001</b>	1.000
Age at adoption, mean (SD), years:months	3:3 (2:8)	2:7 (2:5)	—	—	0.237
Clinical assessment					
(1) Prenatal alcohol exposure (%)					
4. Confirmed, severe	21 (40.4)	16 (43.2)	—	—	0.959
3. Confirmed, moderate or unquantified	26 (50.0)	19 (51.1)	—	—	1.000
2. Not documented	5 (9.6)	2 (5.4)	—	—	0.743
(2) FAS facial features (%)					
4. Severe	31 (59.6)	2 (5.4)	—	—	<b>&lt;0.001</b>
3. Moderate	21 (40.3)	1 (2.7)	—	—	<b>&lt;0.001</b>
2. Mild	0 (0.0)	30 (81.1)	—	—	<b>&lt;0.001</b>
1. None	0 (0.0)	4 (10.8)	—	—	0.057
(3) Growth deficiency (%)					
4. Significant	19 (36.5)	3 (8.1)	—	—	<b>0.005</b>
3. Moderate	11 (21.2)	2 (5.4)	—	—	0.077
2. Mild	9 (17.3)	9 (24.3)	—	—	0.586
1. None	13 (25.0)	23 (62.2)	—	—	<b>0.001</b>
Brain anatomy					
Head circumference, smallest known (%)					
≤ -2 SD: microcephaly	34 (65.4)	13 (35.1)	—	—	<i>0.009</i>
< 10th centile	46 (88.5)	21 (56.8)	—	—	<b>0.002</b>
Structural brain anomalies from first radiologist report (%)					
Corpus callosum abnormality	9 (17.3)	5 (13.5)	—	—	0.850
Cerebellum abnormality	7 (13.5)	5 (13.5)	—	—	1.000
Nodular heterotopia	2 (3.8)	0 (0.0)	—	—	0.630
Agenetic/punctiform olfactory bulb	2 (3.8)	1 (2.7)	—	—	1.000
(4) Structural brain damage (%)	40 (76.9)	19 (51.4)	—	—	0.290
Functional brain assessment					
IQ median (10th centile)	<i>n</i> = 39; 80 (65.8)	<i>n</i> = 30; 79 (64.0)	—	—	/
GAI median (10th centile)	<i>n</i> = 43; 82 (64.2)	<i>n</i> = 29; 86 (68.2)	—	—	/
(4) Brain damage (%)					
4. Certain	39 (75.0)	15 (40.5)	—	—	<b>0.002</b>
3. Probable	13 (25.0)	17 (45.9)	—	—	0.067
2. Possible	0 (0.0)	5 (13.5)	—	—	<i>0.024</i>
Discordant diagnostic with revised Institute of Medicine guidelines	2 (3.8)	4 (10.8)	—	—	
Cohen's Kappa coefficient	$\kappa = 0.86$				

Four diagnostic criteria of the 4-Digit Diagnostic Code described in Figure S1. Concordance between the two guidelines (Cohen's Kappa coefficient,  $\kappa$ ).

Bold type,  $p < 0.007$ , after Bonferroni correction; italic type,  $p < 0.05$ .

Abbreviations: FAS, fetal alcohol syndrome; FASD, fetal alcohol spectrum disorder; NS-FASD, non-syndromic fetal alcohol spectrum disorder; GAI, General Ability Index; SD, standard deviation.

<sup>a</sup> $p$ -value from analysis of variance ( $F$ -test) or proportion test.

<sup>b</sup> $p$ -value from Student's  $t$ -test or  $\chi^2$  test.

**TABLE 2** Neuroanatomical quantitative measurements of brain size, corpus callosum length and thicknesses, and vermis height (group comparison and sex effect on group comparison)

	FAS <i>n</i> = 52	NS-FASD <i>n</i> = 37	Typically developing <i>n</i> = 94	Group effect, <i>p</i> <sup>a</sup>	Sex effect, <i>p</i> <sup>a</sup>	FAS vs NS-FASD, <i>p</i> <sup>b</sup>
Brain size, mean in cm <sup>2</sup> (SD)						
Reference brain area	160.5 (11.7)	167.1 (12.2)	184.6 (11.1)	<b>&lt;0.001</b>	0.138	<i>0.013</i>
Corpus callosum, mean in mm (SD)						
Length of the corpus callosum	76.7 (11.9)	79.8 (6.0)	86.8 (6.5)	<b>&lt;0.001</b>	0.703	0.104
Genu thickness	10.0 (1.4)	10.6 (1.5)	10.6 (1.5)	0.063	0.904	0.071
Body thickness	5.9 (1.3)	6.4 (1.0)	6.6 (1.0)	<b>0.003</b>	0.361	0.098
Isthmus thickness	3.4 (1.0)	3.9 (0.8)	4.3 (0.9)	<b>&lt;0.001</b>	0.138	<i>0.037</i>
Splenium thickness	9.2 (2.6)	10.4 (1.5)	10.5 (1.4)	<b>&lt;0.001</b>	0.544	<i>0.008</i>
Vermis, mean in mm (SD)						
Height of the vermis	41.5 (5.0)	44.5 (4.0)	46.1 (3.0)	<b>&lt;0.001</b>	0.546	<b>0.002</b>

Bold type,  $p < 0.007$ , after Bonferroni correction; italic type,  $p < 0.05$ .

Abbreviations: FAS, fetal alcohol syndrome; NS-FASD, non-syndromic fetal alcohol spectrum disorder; SD, standard deviation.

<sup>a</sup> $p$ -value from analysis of variance ( $F$ -test).

<sup>b</sup> $p$ -value from Student's  $t$ -test.

(Figure 3a) and there was an excess of individuals with FAS with an abnormally small length of the corpus callosum, isthmus thickness, splenium thickness, and height of the vermis measurements for age ( $p < 0.001$  and  $p = 0.002$  for splenium thickness) (Table 3).

### Scaling anomalies: individual measurements as a function of brain size

To identify anomalies independent of the overall brain size deficit (RBA), we established scaling curves for comparison individuals. The only measurement significantly correlated with brain size was length of the corpus callosum ( $p < 0.001$ ;  $R^2 = 20.4\%$ ), with a trend for body thickness, splenium thickness, and height of the vermis ( $p = 0.012$ ,  $p = 0.020$ ,  $p = 0.023$ ;  $R^2 = 6.6\%$ ,  $5.7\%$ ,  $5.4\%$  respectively) (Figure S3). There was an excess of individuals with FAS below the 10th centile for isthmus thickness and height of the vermis only ( $p = 0.003$  after excluding the two with ACC,  $p < 0.001$  respectively) (Table 3 and Figure 3b,c), which was also found in the alternative analysis separating females and males (Figure S4).

### Semi-quantitative assessment of the upper vermis foliation

The agreement along the five-rank scale between the three observers was moderate ( $\kappa = 0.44$ ) but increased to strong ( $\kappa = 0.65$ ) when it came to differentiating individuals with 'not very typical' or 'not at all typical' foliation (4 or 5) from the others, with no comparison individual ever ranked 4 or 5 (Figure S5). Eleven individuals ranked 4 (eight with FAS, three with NS-FASD) and five ranked 5 (three with FAS, two with NS-FASD), totalling 18.0% considered to have

disrupted upper vermis foliation. Notably, four individuals who ranked 4 or 5 did not show a small vermis for brain size (Figure 3c, blue points), making this semi-quantitative assessment non-redundant with height of the vermis.

### Combination of neuroanatomical abnormalities

We identified four recurrent neuroanatomical abnormalities in FAS not trivially associated with each other and particularly not plain consequences of brain size deficit, illustrated in Figure 4.

We grouped the clinical and radiological evidence of FAS-related neuroanatomical damage as follows: (1) brain size deficit for age—clinically (head circumference) and/or radiologically (RBA); (2) corpus callosum abnormalities—partial ACC or narrowed callosal isthmus for brain size; (3) vermis abnormalities—disrupted upper vermis foliation and/or insufficient vermian height for brain size.

There were 38.5% with FAS, 27.0% with NS-FASD, and only 2.1% of comparison individuals with two out of these three abnormalities, and 19.2% with FAS with all three (Table 4), showing both a discriminative value of the association of FAS-recurrent neuroanatomical abnormalities and its possible observation in NS-FASD.

### Integration into a neuroanatomical criterion

A diagnostic tree, including a distinct and quantified neuroanatomical criterion that gives double weight to the well-documented and frequent brain size deficiency, is proposed in Figure 5. An assumption of the strength of the causal link with PAE is associated with each combination of non-facial criteria within each tree branch. We found



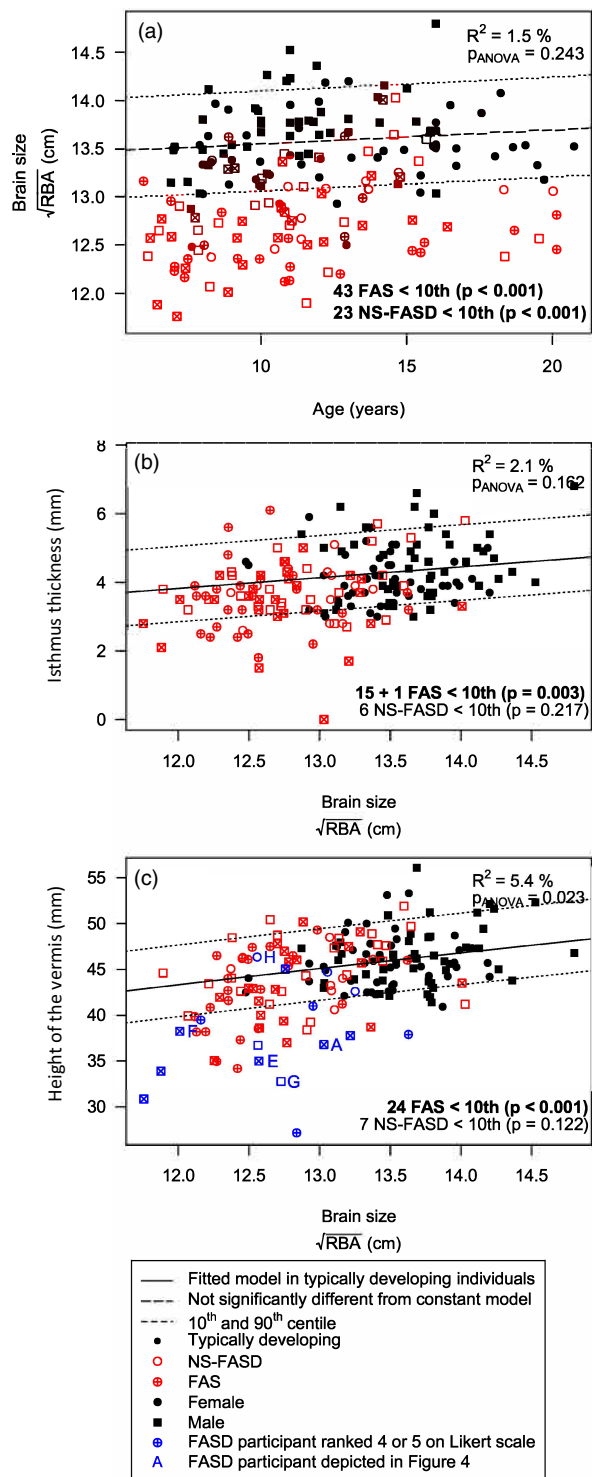


**FIGURE 3** Fetal alcohol syndrome (FAS)-recurrent abnormal measurements. (a) Growth chart for brain size. (b,c) Scaling charts for isthmus thickness and the height of the vermis. Top: determination coefficient  $R^2$  and  $p_{ANOVA}$  ( $p$ -value of comparison of fitted model vs constant) in comparison individuals. Bottom: number of fetal alcohol spectrum disorder (FASD) < 10th centile ( $p$ -value of one-sided Fisher's test). Bold type,  $p < 0.007$ .

that 18.0% of participants with NS-FASD were associated with high levels of causal link with PAE (very likely, almost certain).

## DISCUSSION

In this study, we have described recurrent excessive narrowing of the callosal isthmus and insufficient vermian height associated with FAS, not explained by brain size deficit, using validated neuroanatomical measurements<sup>20,21</sup> that are accessible in a clinical–radiological setting on routine T1-weighted MRI. We also introduced a simple and reliable tool to evaluate the foliation of the upper vermis and showed its usefulness in identifying disrupted foliation associated with FAS, never observed in typically developing comparison individuals, and not always related to insufficient vermian height. Lastly, we demonstrated that the association of two or three of either brain size, callosal or vermian abnormalities was frequent not only in FAS but also in NS-FASD, while remaining exceptional in comparison individuals. These results strongly favour the addition of a composite neuroanatomical criterion to the current FASD clinical diagnostic procedure, including specified and objective radiological assessment, as it can improve the estimation of the causal link with PAE and open the path to a better diagnostic specificity in the absence of FAS.

### Accounting for brain size

Brain size deficit is the most obvious and recurrent neuroanatomical abnormality in individuals with FASD.<sup>1,8,9</sup> The head circumference has shown only a moderate correlation to the actual brain volume in the typically developing and the PAE populations beyond the age of 6 years ( $R^2 = 36\text{--}43\%$ ).<sup>8</sup> As brain volume is not yet easily accessible in routine MRI, we proposed the measurement of RBA as a useful radiological proxy of brain size, strongly correlated with it ( $R^2 = 74.9\%$ ; Figure S2) and geometrically more sensitive than length or perimeter.<sup>8</sup> Associating RBA with present or former clinical measurements of head circumference<sup>18</sup> would eventually increase the sensitivity of detection of brain growth deficiency.

Brain size must be considered when interpreting other neuroanatomical measurements that correlate with it in the general population<sup>24</sup> and thus are plainly reduced in small brains. Thus, to interpret the reduction in callosal and vermian size observed in FASD at the individual level, we complemented the classical normative analysis on growth charts (effect of age) with an analysis on scaling charts (effect of size). Because of the partial overlap between FASD and comparison individuals' ranges of brain sizes, we had to ensure that the scaling model fitted in comparison individuals correctly projected to the smaller FASD range. Allometric scaling modelled by a power law captures the gradual change in proportions along size range and has been shown to be the rule rather than the exception in neuroanatomy.<sup>16,22</sup> Not taking it into account can be misleading<sup>25</sup> and, in our situation, a simple affine model would have dubiously increased abnormal FASD measurements, whereas the power-law model is more conservative. Lastly, most of the participants with FASD with

**TABLE 3** Number of participants with FASD below the 10th centile on growth and scaling normative charts established in comparison individuals for each measured parameter

FASD <i>n</i> = 89	Growth				Scaling			
	FAS <10th centile	<i>p</i>	NS-FASD <10th centile	<i>p</i>	FAS <10th centile	<i>p</i>	NS-FASD <10th centile	<i>p</i>
Brain size								
Reference brain area	43	<0.001	23	<0.001				
Corpus callosum								
Length of the corpus callosum	27 (+2)	<0.001	17	<0.001	7 (+2)	0.294	4	0.529
Genu thickness	10	0.082	5	0.354	3	0.870	3	0.715
Body thickness	13 (+1)	0.012	7	0.122	6 (+1)	0.440	2	0.873
Isthmus thickness	20 (+1)	<0.001	9	0.031	15 (+1)	<b>0.003</b>	6	0.217
Splenium thickness	15 (+2)	<b>0.002</b>	4	0.529	9 (+2)	0.118	0	1.000
Vermis								
Height of the vermis	32	<0.001	9	0.031	24	<0.001	7	0.122

*p*-value from one-sided Fisher's test. In brackets, the excluded individuals with agenesis of corpus callosum. Bold type,  $p < 0.007$ , after Bonferroni correction; italic type,  $p < 0.05$ . For the charts used to establish these results, see Figure S3.

Abbreviations: FAS, fetal alcohol syndrome; FASD, fetal alcohol spectrum disorder; NS-FASD, non-syndromic fetal alcohol spectrum disorder.

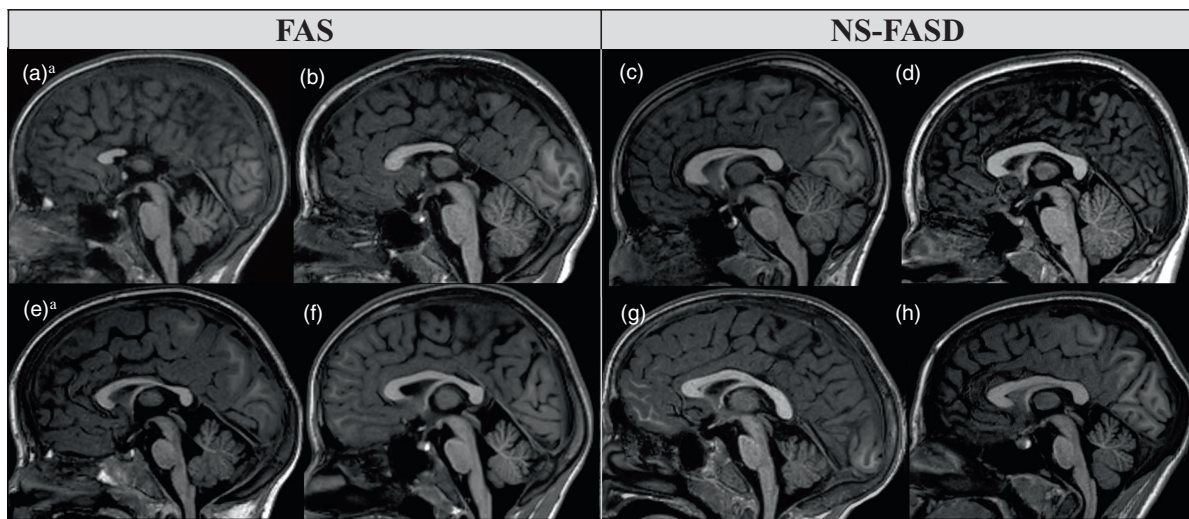


**FIGURE 4** Individuals with fetal alcohol spectrum disorder (FASD) with identified fetal alcohol spectrum (FAS)-recurrent anomalies. (a,b) Partial agenesis of corpus callosum. (c,d) Narrowed callosal isthmus for brain size. (e,g) Upper vermis ranked 5; (f,h) ranked 4. Note that for (h) the height of the vermis is normal for brain size (Figure 3). <sup>a</sup> Association of three abnormalities.

either vermian or callosal measurements too small for age showed normal values for brain size, as was flagrant for the length of the corpus callosum (Table 3). The reduction of isthmus thickness and height of the vermis were the only ones not strictly redundant with brain size reduction. In terms of non-redundancy of abnormal features, we also showed that disrupted upper foliation could be found in a normal-sized vermis (Figure 3c, individual H). Ultimately, this scaling normative approach helped discover abnormalities that were complementary enough to be combined with brain size deficit within an FAS neuroanatomical pattern and possible diagnostic criterion.

### Specificity of the abnormalities

We identified frequent height (44.9%) and/or foliation (18.0%) vermian abnormalities. Surprisingly, this result was not highlighted in most published FASD clinical-radiological studies,<sup>11,26</sup> except in a recent qualitative large series,<sup>10</sup> though that study provided little description. Yet, several computer-assisted neuroimaging studies have reported a size reduction of the anterior vermis (area, volume) following PAE<sup>7,15,17</sup> at the group level, generally taking brain size effect linearly into account. Our results suggest that there might also be a qualitative disruption of vermian foliation

**TABLE 4** Recurrent neuroanatomical abnormalities identified in FAS, counted in each group FAS, NS-FASD, and combination of two or three of the abnormalities, versus comparison individuals

	FAS	<i>p</i>	NS-FASD	<i>p</i>	Typically developing
<b>Recurrent neuroanatomical abnormalities</b>					
Brain size deficit					
Reference brain area < 10th centile and/or head circumference < 10th centile	48 (92.3%)	<b>&lt;0.001</b>	27 (73.0%)	<b>&lt;0.001</b>	9 (9.6%)
Corpus callosum abnormalities					
Partial ACC and/or narrowed callosal isthmus (isthmus thickness < 10th centile)	17 (32.7%)	<b>0.001</b>	6 (16.2%)	0.217	9 (9.6%)
Vermis abnormalities					
Insufficient vermian height (<10th centile)	25 (48.1%)	<b>&lt;0.001</b>	10 (27.0%)	<i>0.014</i>	9 (9.6%)
Disrupted upper vermis foliation (Likert 4, 5)	24		7		9 (9.6%)
	11		5		0 (0.0%)
<b>Combination of neuroanatomical abnormalities</b>					
Brain size deficit associated with corpus callosum or vermis abnormalities	20 (38.5%)	<b>&lt;0.001</b>	10 (27.0%)	<b>&lt;0.001</b>	2 (2.1%)
Brain size deficit associated with corpus callosum and vermis abnormalities	10 (19.2%)	<b>&lt;0.001</b>	0 (0.0%)	1.000	0 (0.0%)

*p*-value from one-sided Fisher's test. Bold type, *p* < 0.007, after Bonferroni correction; italic type, *p* < 0.05.

Abbreviations: ACC, agenesis of corpus callosum; FAS, fetal alcohol syndrome; NS-FASD, non-syndromic fetal alcohol spectrum disorder.

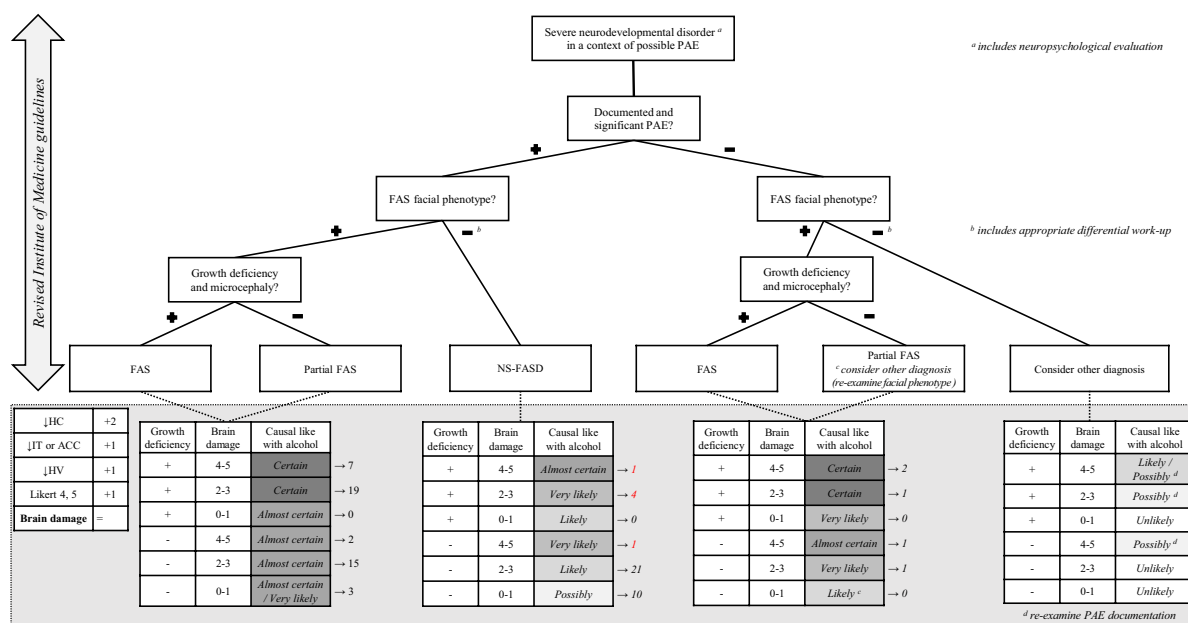


**FIGURE 5** Proposition of revised FASD diagnostic algorithm (based on the revised Institute of Medicine guidelines) with an estimate of the probability of a causal link between clinical phenotype and PAE, based on documentation of consumption, FAS facial phenotype, growth deficiency, as well as a specified neuroanatomical criterion as a 'brain damage' score: brain growth deficiency (↓HC), ACC or narrowing of the callosal isthmus for brain size (↓IT) and insufficient vermian height for brain size (↓HV) or disrupted upper vermis foliation (Likert 4, 5). Number of participants with FASD in each category noted on the right; red type, high level of probability in participants with NS-FASD. Abbreviations: ACC, agenesis of corpus callosum; FAS, fetal alcohol syndrome; FASD, fetal alcohol spectrum disorder; HC, head circumference; HV, height of the vermis; IT, isthmus thickness; NS-FASD, non-syndromic fetal alcohol spectrum disorder; PAE, prenatal alcohol exposure.

(branching, length, thickness of the folia). The Likert scale we propose was based on the formalism adopted in the literature for FASD facial morphology.<sup>5,6</sup> Under the proposed conditions, ranking 1, 2, or 3 is not very robust, but the relevance of this scale is supported by the strong agreement

between observers in distinguishing typical from atypical aspects that should be considered pathological, without misclassification of comparison individuals. Indeed, as for facial morphology, it is the distinction of the two pathological ranks that is relevant to clinical use, and the effectiveness

of the Likert scale probably relies on its spreading over five ranks.

In FASD, cases of ACC have been repeatedly reported.<sup>7,10,11</sup> In these three large recent cohorts, the prevalence of ACC did not exceed 3% (2.2% in ours), while it is rated from 0.02% to 0.7% in the general population<sup>27</sup> to around 1% in individuals with neurodevelopmental disorders.<sup>28</sup> Qualitatively abnormal or atypical shapes may be reported in up to 38% of cases,<sup>10</sup> but criteria are subjective and difficult to interpret. Using computerized analysis tools, subtle anomalies were found at the group level: differences in volume, surface, length, or position<sup>12–14</sup> versus typically developing individuals. Unfortunately, these results are heterogeneous or difficult to replicate.<sup>12,29</sup> We found a clear excess of abnormally thin isthmus. Considering the reports of posterior partial ACC and possibly of splenic anomalies at the group level, we expected to find a similar excess of narrowed splenium, but it was not significant in our population. Despite well-codified measurement criteria,<sup>20</sup> the complex shape variability of the splenium (rounded, curved, short without being thin) may have limited the sensitivity of abnormality detection.

To our knowledge, none of the previous studies on callosal and vermian abnormalities have so far attempted to propose any practical and normative use at the individual level.

### Interest of a neuroanatomical diagnostic criterion

Over time, the evolution of FASD diagnostic guidelines has given variable importance to neuroanatomical features, sometimes discounting them,<sup>4</sup> often mixing them with neurofunctional impairment,<sup>3,5,6</sup> always with little, if any, impact on diagnostic specificity. Yet, the triple association of the FAS-recurrent abnormalities we described was repeatedly observed in FAS (19.2%), the double associations were frequent in FAS (38.5%), and repeatedly observed in NS-FASD (27.0%), while both situations were either unobserved or exceptional (2.1%) in typically developing individuals (Table 3). Provided that FAS-specificity and extendibility to some NS-FASD are confirmed by other large-scale studies, such a brain signature could form the basis of a specified and independent neuroanatomical diagnostic criterion that would be worth discussing beyond a simply descriptive value (Figure 5). Within the framework of existing diagnostic categories and respecting the preeminent specificity of the facial phenotype, we showed that adding this type of criterion can help refine the estimation of the probabilistic link between neurodevelopmental disorders and PAE, and contribute to identify a sub-category of NS-FASD in which this estimated link is particularly strong. Thus, without being indispensable in cases sufficiently supported by the clinic, brain MRI could find its place in the diagnostic work-up when a strengthening of the probabilistic diagnosis of FASD-NS is desirable.

### Limitations

As for any retrospective study on FASD,<sup>10,11,29</sup> the representativeness of the population is an important issue. In this regard, our series included a high proportion of adopted children (60.7%) for whom PAE was documented but poorly quantified and perinatal comorbidities were difficult to exclude.

One could question the way the 10th centile of the scaling curves was established for normative analysis. First, we relied on a power-law scaling model, the most theoretically correct choice,<sup>22,23</sup> which allows for both nonlinear allometric and linear proportional relationships ( $P = b \times \sqrt{RBA}^{a-1}$ ). Yet, low coefficients of determination  $R^2$  associated with a moderate population size ( $n = 94$ ) probably limited the statistical power to assess model fits. That said, keeping a very general model seemed appropriate as it tended to best fit for many parameters before Bonferroni correction and proved to be more conservative (limiting false positives). Finally, to robustly establish the centiles of the distributions in our medium-sized comparison group, we had to assume homogeneous variance over the studied intervals.

The absence of sex distinction, even if sex effect on brain size is well known,<sup>8,18</sup> might also be questioned. In this study, pooling males and females resulted from a trade-off between statistical power and robustness (model fit) linked to the size of the comparison group, and adequacy of normative limits at the individual level (charts) brought by adding the sex covariate. We explored the extent to which this choice would affect our results and first verified that there was no significant effect of sex on the raw measurements excepted for brain size (Table 2), which was consistent with the strongly negative allometric relationship between brain size and these parameters<sup>22</sup> (significant variations of RBA between males and females, associated with very subtle or insignificant variations of callosal and vermian measurements; Table S1). Bearing in mind that the analyses would be less robust, we also showed that the alternative choice of separating males and females did not significantly change our final results, with concordant identification of both FAS-related neuroanatomical abnormalities (Figure S4) and participants with pathological FASD on the normative charts. In the end, the use of a common growth chart for RBA potentially caused only three false negatives in males and one false positive in females (Figure 3 vs Figure S4), which would have been counted as one FAS and two NS-FASD with a combination of two anomalies, thus not changing the conclusions.

The choice of a 10th centile thresholding over a lower one is also questionable, especially because it has been a source of controversy in the field<sup>30</sup> for other diagnostic parameters. Since we intended to combine the abnormalities, we considered that this threshold would not be too permissive in the end, which proved to be correct as double or triple combinations dropped almost below the detection level in about 100 typically developing individuals. Eventually, a third centile-threshold alternative analysis consistently showed a significant excess of isthmus thickness and height of the vermian abnormality for brain size (data not shown).



All these concerns advocate complementary studies for more accurate standardization of the scaling curves, including sex differentiation and extending age ranges to adult charts, taking advantage of larger samples or multisite designs. However, the relatively large excess of abnormal isthmus thickness and height of the vermis values with a nonetheless conservative model gives us confidence in our results.

## CONCLUSION

Explicit and quantitative FAS-recurrent anomalies (small brain size for age, narrowed callosal isthmus for brain size, and disrupted upper vermis foliation or reduced vermian height for brain size) can be associated into a composite neuroanatomical–radiological criterion. It is likely to benefit the diagnostic process for NS-FASD, bringing confidence where some lack of specificity can deter diagnosis, for the sake of diagnosis rate and eventually patient care.

## ACKNOWLEDGMENTS

We thank the volunteers, patients, and families, the French supportive association for FASD-affected families ‘*Vivre avec le SAF*’, and Elizabeth Rowley-Jolivet for English proofreading.

## FUNDING INFORMATION

The French National Agency for Research (ANR-19-CE17-0028-01) and the French National Institute for Public Health research (IRESP-19-ADDICTIONS-08).

## CONFLICT OF INTEREST

The authors have stated that they had no interests that might be perceived as posing a conflict or bias.

## DATA AVAILABILITY STATEMENT

The data that support the findings of this study are available on request from the corresponding author. The data are not publicly available due to privacy or ethical restrictions.

## ORCID

Justine Fraize  <https://orcid.org/0000-0001-6434-7992>

## REFERENCES

- Kuehn D, Aros S, Cassorla F, Avaria M, Unanue N, Henriquez C, et al. A prospective cohort study of the prevalence of growth, facial, and central nervous system abnormalities in children with heavy prenatal alcohol exposure. *Alcohol Clin Exp Res*. 2012; 36(10):1811–9.
- Lange S, Probst C, Gmel G, Rehm J, Burd L, Popova S. Global Prevalence of Fetal Alcohol Spectrum Disorder Among Children and Youth: A Systematic Review and Meta-analysis. *JAMA Pediatr*. 2017; 171(10):948–956.
- Chudley AE. Diagnosis of fetal alcohol spectrum disorder: current practices and future considerations. *Biochem Cell Biol*. 2018; 96(2):231–236.
- Cook JL, Green CR, Lilley CM, Anderson SM, Baldwin ME, Chudley AE, et al. Fetal alcohol spectrum disorder: a guideline for diagnosis across the lifespan. *CMAJ*. 2016; 188(3):191–197.
- Astley SJ. *Diagnostic Guide for Fetal Alcohol Spectrum Disorders: The 4-Digit Diagnostic Code*. 3rd edition University of Washington Publication Services, Seattle, WA: 2004. Available from: <http://depts.washington.edu/fasdpn/pdfs/guide04.pdf>
- Hoyme HE, Kalberg WO, Elliott AJ, Blankenship J, Buckley D, Marais AS, et al. Updated Clinical Guidelines for Diagnosing Fetal Alcohol Spectrum Disorders. *Pediatrics*. 2016; 138(2):e20154256.
- Astley SJ, Aylward EH, Olson HC, Kerns K, Brooks A, Coggins TE, et al. Magnetic resonance imaging outcomes from a comprehensive magnetic resonance study of children with fetal alcohol spectrum disorders. *Alcohol Clin Exp Res*. 2009; 33(10):1671–89.
- Treit S, Zhou D, Chudley AE, Andrew G, Rasmussen C, Nikkel SM, et al. Relationships between Head Circumference, Brain Volume and Cognition in Children with Prenatal Alcohol Exposure. *PLoS One*. 2016; 11(2):e0150370.
- Nguyen VT, Chong S, Tieng QM, Mardon K, Galloway GJ, Kurniawan ND. Radiological studies of fetal alcohol spectrum disorders in humans and animal models: An updated comprehensive review. *Magn Reson Imaging*. 2017; 43:10–26.
- Boronat S, Sánchez-Montañez A, Gómez-Barros N, Jacas C, Martínez-Ribot L, Vázquez E, et al. Correlation between morphological MRI findings and specific diagnostic categories in fetal alcohol spectrum disorders. *Eur J Med Genet*. 2017; 60(1):65–71.
- Treit S, Jeffery D, Beaulieu C, Emery D. Radiological Findings on Structural Magnetic Resonance Imaging in Fetal Alcohol Spectrum Disorders and Healthy Controls. *Alcohol Clin Exp Res*. 2020; 44(2):455–462.
- Sowell ER, Mattson SN, Thompson PM, Jernigan TL, Riley EP, Toga AW. Mapping callosal morphology and cognitive correlates: effects of heavy prenatal alcohol exposure. *Neurology*. 2001; 57(2):235–244.
- Bookstein FL, Connor PD, Huggins JE, Barr HM, Pimentel KD, Streissguth AP. Many infants prenatally exposed to high levels of alcohol show one particular anomaly of the corpus callosum. *Alcohol Clin Exp Res*. 2007; 31(5):868–879.
- Biffen SC, Warton CMR, Dodge NC, Molteno CD, Jacobson JL, Jacobson SW, et al. Validity of automated FreeSurfer segmentation compared to manual tracing in detecting prenatal alcohol exposure-related subcortical and corpus callosal alterations in 9- to 11-year-old children. *Neuroimage Clin*. 2020; 28:102368.
- O'Hare ED, Kan E, Yoshii J, Mattson SN, Riley EP, Thompson PM, et al. Mapping cerebellar vermal morphology and cognitive correlates in prenatal alcohol exposure. *Neuroreport*. 2005; 16(12):1285–90.
- Bookstein FL, Streissguth AP, Connor PD, Sampson PD. Damage to the human cerebellum from prenatal alcohol exposure: the anatomy of a simple biometrical explanation. *Anat Rec B New Anat*. 2006; 289(5):195–209.
- Cardenas VA, Price M, Infante MA, Moore EM, Mattson SN, Riley EP, et al. Automated cerebellar segmentation: Validation and application to detect smaller volumes in children prenatally exposed to alcohol. *Neuroimage Clin*. 2014; 4:295–301.
- Rollins JD, Collins JS, Holden KR. United States head circumference growth reference charts: birth to 21 years. *J Pediatr*. 2010; 156(6):907–913.e2.
- Bouyeure A, Germanaud D, Bekha D, Delattre V, Lefèvre J, Pinabiaux C, et al. Three-Dimensional Probabilistic Maps of Mesial Temporal Lobe Structures in Children and Adolescents' Brains. *Front Neuroanat*. 2018; 12:98.
- Garel C, Cont I, Alberti C, Josserand E, Moutard ML, Ducou le Pointe H. Biometry of the corpus callosum in children: MR imaging reference data. *AJNR Am J Neuroradiol*. 2011; 32(8):1436–43.
- Jandeaux C, Kuchcinski G, Ternynck C, Riquet A, Leclerc X, Pruvo JP, et al. Biometry of the Cerebellar Vermis and Brain Stem in Children: MR Imaging Reference Data from Measurements in 718 Children. *AJNR Am J Neuroradiol*. 2019; 40(11):1835–1841.
- de Jong LW, Vidal JS, Forsberg LE, Zijdenbos AP, Haight T, Alzheimer's Disease Neuroimaging Initiative, et al. Allometric scaling of brain regions to intra-cranial volume: An epidemiological MRI study. *Hum Brain Mapp*. 2017; 38(1):151–164.
- Germanaud D, Lefèvre J, Fischer C, Bintner M, Curie A, des Portes V, et al. Simplified gyral pattern in severe developmental microcephalies?



- New insights from allometric modeling for spatial and spectral analysis of gyrification. *Neuroimage*. 2014; 102 Pt 2:317–31.
24. Giedd JN, Rapoport JL. Structural MRI of Pediatric Brain Development: What Have We Learned and Where Are We Going? *Neuron*. 2010; 67(5):728–734.
  25. Toro R, Chupin M, Garnero L, Leonard G, Perron M, Pike B, et al. Brain volumes and Val66Met polymorphism of the BDNF gene: local or global effects? *Brain Struct Funct*. 2009; 213(6):501–9.
  26. Autti-Rämö I, Autti T, Korkman M, Kettunen S, Salonen O, Valanne L. MRI findings in children with school problems who had been exposed prenatally to alcohol. *Dev Med Child Neurol*. 2002; 44(2):98–106
  27. Glass HC, Shaw GM, Ma C, Sherr EH. Agenesis of the corpus callosum in California 1983–2003: a population-based study. *Am J Med Genet A*. 2008; 146A(19):2495–2500.
  28. Jeret JS, Serur D, Wisniewski K, Fisch C. Frequency of agenesis of the corpus callosum in the developmentally disabled population as determined by computerized tomography. *Pediatr Neurosci*. 1985; 12(2):101–103.
  29. Yang Y, Phillips OR, Kan E, Sulik KK, Mattson SN, Riley EP, et al. Callosal thickness reductions relate to facial dysmorphology in fetal alcohol spectrum disorders. *Alcohol Clin Exp Res*. 2012; 36(5):798–806.
  30. Hemingway SJA, Bledsoe JM, Brooks A, Davies JK, Jirikowic T, Olson E, et al. Comparison of the 4-Digit Code, Canadian 2015, Australian 2016 and Hoyme 2016 fetal alcohol spectrum disorder diagnostic guidelines. *Adv Pediatr Res*. 2019; 6(2):31.

## SUPPORTING INFORMATION

The following additional material may be found online:

**Figure S1** Flow chart and diagnostic procedure.

**Figure S2** Correlation between reference brain area (RBA) and total brain volume obtained with *volBrain*.

**Figure S3** Growth charts (left), scaling charts (right).

**Figure S4** Charts of female (left) and male (right).

**Figure S5** Semi-quantitative assessment of the upper vermis foliation.

**Table S1** Effect of scanner, age, and sex on measured parameters in the comparison group.

**How to cite this article:** Fraize J, Garzón P, Ntorkou A, Kerdreux E, Boespflug-Tanguy O, Beggiato A, et al. Combining neuroanatomical features to support diagnosis of fetal alcohol spectrum disorders. *Dev Med Child Neurol*. 2022;00:1–12. <https://doi.org/10.1111/dmcn.15411>